Formation of a High Affinity Lipid-Binding Intermediate during the Early Aggregation Phase of α-Synuclein†

David P. Smith,‡,§,# Deborah J. Tew,‡,||,§ Andrew F. Hill,‡,⊥,|| Stephen P. Bottomley,⊗ Colin L. Masters,‡,§ Kevin J. Barnham,‡,||,§ and Roberto Cappai*,‡,||,§

Department of Pathology, Department of Biochemistry and Molecular Biology, Bio21 Molecular Science and Biotechnology Institute, The University of Melbourne, Victoria, 3010, Australia, The Mental Health Research Institute of Victoria, Parkville, Victoria, 3052, Australia, and Department of Biochemistry and Molecular Biology, Monash University, Victoria, 3800, Australia

Received July 30, 2007; Revised Manuscript Received November 12, 2007

ABSTRACT: The α-synuclein (α-syn) protein is clearly implicated in Parkinson's disease (PD). Mutations or triplication of the α-syn gene leads to early onset PD, possibly by accelerating α-syn oligomerization. α-syn interacts with lipids, and this membrane binding activity may relate to its toxic activity. To understand how the α-syn aggregation state affects its lipid binding activity we used surface plasmon resonance to study the interaction of wild-type and mutant α-syn with a charged phospholipid membrane, as a function of its aggregation state. Apparent dissociation constants for α-syn indicated that an intermediate species, present during the lag phase of amyloid formation, binds with an increased affinity to the membrane surface. Formation of this species was dependent upon the rate of fibril formation. Fluorescence anisotropy studies indicate that only upon the formation of amyloid material can α-syn perturb the acyl-chain region of the lipid bilayer. Circular dichroism spectroscopy showed that upon aging, both wild-type and mutant α-syn lose their ability to form lipid-bound α-helical species once they become fibrillar. These results indicate that α-syn forms a high affinity lipid binding intermediate species during fibril formation. Oligomeric α-syn is known to be toxic, and it is feasible that the high affinity binding species described here may correspond to a toxic species involved in PD.

Parkinson's disease (PD[1]) is a progressive neurodegenerative disease characterized pathologically by the presence of intraneuronal Lewy bodies containing amyloidogenic α-synuclein (α-syn) and the loss of dopaminergic neurons in the substantia nigra (*1*). Wild-type α-syn (WT α-syn) is a natively unfolded protein which adopts a partially folded conformation with distinct secondary structural elements upon binding to proteins, lipid, and metals (*2*−*4*). The N-terminal region of α-syn is highly conserved, rich in basic residues and contains six 11-residue repeats with the consensus sequence KTKEGV (*5*). These repeats share homology with the lipid-binding α-helical domain of apolipoproteins and have a propensity to readily form amphipathic α-helices (*5*). When α-syn interacts with acidic phospholipids, it adopts an α-helical conformation (*2*). The C-terminal acidic domain of α-syn is unstructured and truncating this region results in an increased propensity to form amyloid-like fibrils (*3*, *4*, *6*). The self-association of full length α-syn into *β*-sheet oligomers and protofibrils occurs *via* metastable, misfolded intermediates, and accumulation of these oligomeric intermediates may contribute to a toxic gain of function that results in neurodegeneration (*7*).

A number of mutations in the α-syn gene have been associated with early onset PD (*8*). The A53T and E46K mutations increase α-syn fibril assembly (*9*−*12*). In contrast, the A30P mutant has less defined aggregation properties with conflicting studies reporting the aggregation rates of A30P α-syn as unchanged, increased, or decreased (*13*−*15*). These discrepancies may reflect the aggregation rate being dependent upon the conditions used (*13*−*15*). WT and A53T α-syn bind to lipid membranes containing acidic phospholipids with similar affinities, whereas A30P α-syn displays weaker binding (*2*, *3*, *16*−*19*). WT and A53T α-syn can bind to vesicles derived from either homogenized rat brain cells or lipid rafts prepared from HeLa cell membranes, while A30P α-syn has impaired binding activity (*17*, *19*−*22*). The ability of WT α-syn to disrupt membranes of various compositions

† This work was funded in part by the Wellcome Trust (WT069851MA), National Health and Medical Research Council of Australia, Australian Research Council, and the Australian National Health and Medical Research Council (NHMRC). R.C. and K.J.B. are NHMRC Senior Research Fellows. A.F.H. is an NHMRC RD Wright Fellow.

* To whom correspondence should be addressed. Phone (+61-3) 8344-2556. Fax (+61-3) 9347-6750. E-mail r.cappai@unimelb.edu.au.

‡ Department of Pathology, The University of Melbourne.

⊥ Department of Biochemistry and Molecular Biology, The University of Melbourne.

|| Bio21 Molecular Science and Biotechnology Institute, The University of Melbourne.

§ The Mental Health Research Institute of Victoria.

⊗ Department of Biochemistry and Molecular Biology, Monash University.

Current address: Institute of Molecular and Cellular Biology, University of Leeds, Leeds, UK.

[1] Abbreviations: DPH, diphenyl-1,3,5-hexatriene; DMSO, dimethyl sulfoxide; POPC, 1-palmitoyl-2-oleoyl-*sn*-glycero-3-phosphocholine; POPS, 1-palmitoyl-2-oleoyl-*sn*-glycero-3-[phospho-L-serine]; CHAPS, 3-[(3-cholamidopropyl)dimethylammonio]-1-propanesulfonate; α-syn, α-synuclein; EM, electron microscopy; FA, fluorescence anisotropy; PD, Parkinson's disease; SPR, surface plasmon resonance; ThT, thioflavin-T; WT α-syn, wild-type α-synuclein.

10.1021/bi701522m CCC: $40.75
Published on Web 01/08/2008

correlates with its binding affinity (*23*). Moreover, the oligomeric and fibrillar species cause a more rapid disruption of the membrane than does the monomeric form (*23*). Small α-syn oligomers within cells preferentially associate with lipid droplets and cell membranes (*24*), suggesting a possible target for α-syn-mediated pathogenesis is *via* membrane interactions. Defining the specific α-syn oligomeric species that is associated with lipid membranes is important to understand how the α-syn aggregation state relates to its pathophysiological activities. In this study we use surface plasmon resonance (SPR) to show that a transient species, populated during the lag phase of WT α-syn fibril formation, binds to negatively charged synthetic membranes with a 100-fold higher apparent affinity than unaged α-syn. The familial-PD mutations, A53T and A30P, formed fibrils at an increased rate compared to WT α-syn and generated the high affinity binding intermediate at an earlier time point and without an apparent lag phase. Moreover, all three α-syn proteins display an increased ability to form an α-helical structure coinciding with the formation of the high affinity species which is then lost upon the formation of ThT reactive material.

MATERIALS AND METHODS

Expression and Aggregation of Recombinant α-syn. The human WT α-syn coding region was cloned into pRSETB (Invitrogen) and overexpressed in the *E. coli* strain BL21-(DE3) (*25*). The A30P and A53T mutants were synthesized using the Quikchange mutagenesis kit (Stratagene). WT α-syn and the mutants A53T and A30P were purified as described previously (*25*). Amyloid formation was carried out using 400 μL aliquots of 200 μM WT α-syn or its mutants in 10 mM sodium phosphate buffer, pH 7.4. The solution was filtered to ensure removal of preformed aggregates (0.2 μm Minisart RC4 filters, Sartorius) and then incubated at 37 °C with shaking at 200 rpm for 0 to 4 days. Aliquots were removed as required for each of the following experiments.

Lipid Preparation. Small (50 nm) unilamellar vesicles (SUV) of 50% 1-palmitoyl-2-oleoyl-*sn*-glycero-3-phosphocholine (POPC) and 50% 1-palmitoyl-2-oleoyl-*sn*-glycero-3-[phospho-L-serine] (POPS) (Avanti, Polar Lipids) were prepared in 10 mM sodium phosphate, pH 7.4, by sonication and extrusion. Dry POPC and POPS were dissolved in ethanol-free chloroform (1:1 mol/mol), and the the solvent was evaporated and dried under a stream of nitrogen. The lipids were resuspended in 10 mM sodium phosphate, pH 7.4, *via* mixing for 1 h at 37 °C at 200 rpm in the presence of glass beads. The resultant lipid dispersion, at a concentration of 1 mM, was sonicated in a soncating water bath for 15 min and extruded 17 times, first through a 100 nm pore size polycarbonate filter and then a 50 nm to obtain SUV at 50 nm size (Millipore) and used to prepare the lipid bilayer system. For the preparation of LUV (large unilamellar vesicles), the resultant lipid dispersion subjected to five freeze−thaw cycles using liquid nitrogen and a 37 °C water bath. The solution was extruded 11 times through a 0.1 μm pore filter (Millipore) using an Avanti "mini-extruder" apparatus. LUV were stored at 4 °C and used within 24 h of preparation.

Surface Plasmon Resonance Experiments. All binding experiments were performed on a BIACORE 1000 apparatus using the L1 sensor chip (Biacore AB, Uppsala, Sweden). The L1 sensor chip (Biacore) was composed of alkyl chains covalently linked to a dextran-coated gold surface. The running buffer was 10 mM sodium phosphate, pH 7.4, the wash solution was 40 mM 3-[(3-cholamidopropyl)dimethylammonio]-1-propanesulfonate (CHAPS), and the regeneration solution was 10 mM sodium hydroxide, 100 mM sodium chloride. All solutions were freshly prepared, degassed, and filtered through a 0.22 μm filter (Sartorius).

The surface of the L1 Sensor Chip was cleaned by two injections of the non-ionic detergent 40 mM CHAPS (50 μL) at a flow rate of 100 μL/min. SUV were applied to the sensor chip surface at a flow rate of 2 μL/min in the presence of 0.1 mM NaCl. To remove any multilamellar structures from the lipid surface, 30 μL of 10 mM sodium hydroxide was injected at a flow rate of 50 μL/min. The surface was conditioned four times before use by injecting of 50 μL of BSA at 1 mg/mL at a flow rate of 10 μL/min followed by a 60 μL injection of 10 μM α-syn solution at a flow rate of 10 μL/min prepared as above. The sample was premixed before injection. The surface was regenerated with a 50 μL injection of regeneration solution at a flow rate of 50 μL/min. All experiments were carried out at 37 °C.

Solutions of WT or mutant α-syn at 200 μM were prepared as above and incubated for 0 to 4 days. Each sample was serially diluted with a 10 mM sodium phosphate buffer pH 7.4 at concentrations ranging from 200 to 1.5 μM. Buffer blanks were included as controls. The solutions were premixed to resuspend any aggregate, and 60 μL was injected over the lipid surface at a flow rate of 10 μL/min. The protein solution was replaced with running buffer and allowed to dissociate for 300 s. Associated protein left on the lipid surface was removed by a 50 μL injection of the regenerating solution at a flow rate of 50 μL/min.

Circular Dichroism. The CD spectra were obtained using a Jasco 810 spectropolarimeter at 37 °C. Far-UV CD spectra were obtained from 185 to 260 nm with a 0.1 cm path length quartz cuvette containing protein at 15 μM in the presence or absence of 4 mM POPC/POPS LUV. The spectral contributions of buffer and LUVs were subtracted as appropriate. Data is reported as mean residue ellipticities, degrees cm^2 $dmol^{-1}$ $residue^{-1}$. Data were analyzed using the CDSSTR algorithm from the Dicroweb website, available at http://public-1.cryst.bbk.ac.uk/cdweb/html/ (*26*, *27*).

Thioflavin-T (ThT) Binding. For determination of fibril growth a discontinuous assay was used. Samples (20 μL) were removed from each sample and added to 600 μL of a 20 μM ThT solution at pH 7.4 in 10 mM sodium phosphate pH 7.4. The ThT fluorescence was quantified on a Varian Eclipse fluorescence spectrophotometer at 37 °C by exciting at 444 nm and scanning the emission wavelengths from 460 to 550 nm with slit widths set at 5 nm. Data was normalized by taking the signal of the buffer alone at 480 nm as unity.

Electron Microscopy. Aliquots (10 μL) of protein at 200 μM were taken at each time point. Carbon-coated copper electron microscopy (EM) grids (ProSci Tech) were coated with protein samples and stained as described (*28*). Grids were viewed on a Siemens 102 transmission electron microscope, operating with a voltage of 60 kV.

Steady-State Polarization of DPH. DPH (diphenyl-1,3,5-hexatriene) was purchased from Molecular Probes. Briefly DPH was dissolved at 10 mM in DMSO and diluted to 16.6

μM in 10 mM sodium phosphate, pH 7.4, containing 416 μM LUV. A 60 μL aliquot of this sample was mixed with 40 μL of α-syn at 10 μM giving final concentrations of 10 μM probe, 250 μM LUV, and 4 μM protein. Samples were then incubated at 37 °C with agitation at 200 rpm for 20 min prior to reading. The dye was excited at 359 nm and emission was recorded at 430 nm. Anisotropy was measured on a Varian Eclipse spectrophotometer using internal polarizers and calculated by the equation: $r = (\mathrm{Ivv} - \mathrm{G.Ivh})/(\mathrm{Ivv} + 2\mathrm{G.Ivh})$, where Ivv and Ivh are the fluorescence intensities when the excitation and emission polarizers are set at v (vertical) and h (horizontal), respectively. The grating factor $G = \mathrm{Ihv/Ihh}$.

Gel Permeation Chromatography. Prepacked Superdex 75 column (Amersham) was equilibrated in 10 mM sodium phosphate buffer, pH 7.4, before loading 200 μM wild type α-syn, A53T or A30P its mutants. A flow rate of 0.5 mL/min was maintained with a BioRad BioLogic workstation. The elutant was monitored using the absorbance at A_{280} nm. The columns were calibrated in 10 mM sodium phosphate buffer, pH 7.4, with blue dextran (220 kDa), bovine serum albumin (66 kDa), carbonic anhydrase (29 kDa), cytochrome c (12.4 kDa), and aprotinin (6.5 kDa).

RESULTS

Establishing the Aggregation Properties of WT and Mutant α-syn. Since this study is investigating the relationship between α-syn aggregation state and lipid binding, we first established the aggregation profiles of WT, A53T, and A30P α-syn over time by measuring amyloid formation using ThT fluorescence and negative stain electron microscopy (EM). Aliquots (200 μM) of α-syn were incubated at 37 °C with agitation at 200 rpm for 4 days in 10 mM sodium phosphate buffer at pH 7.4. Initial samples were subjected to analysis by gel permeation chromatography and indicated that the protein immediately following filtration through a 0.2 μm filter is monomeric. The major peak migrated with an elution volume of 10.0 mL and was consistent with an approximate mass of ~42 kDa, as measured against the globular protein standards. However, because of the unstructured nature of α-syn, it is expected to have a higher hydrodynamic radius than globular proteins of the same MW, and hence this peak most likely represents the monomeric protein (Supporting Information Figure 1). Under these conditions, WT α-syn displayed a 2 day lag phase as monitored by ThT fluorescence (Figure 1, squares), during which small, ~ 10 nm, spherical aggregates were formed (Figure 2). At day 3, the fibrils were surrounded by amorphous aggregates (Figure 2) and this coincided with an increase in ThT fluorescence (Figure 1). In contrast, A53T α-syn had a significantly reduced lag phase of less than 1 day (Figure 1, circles) and formed small spherical aggregates at day 1 which converted to fibrils by day 2 (Figure 2) with a corresponding increase in ThT fluorescence (Figure 1) consistent with previous reports (*29*). The morphologies of the A53T α-syn aggregates at day 1 and 2 were comparable to the WT α-syn forms seen on day 3 and 4. This supports the hypothesis that the aggregation of A53T α-syn is accelerated in comparison to WT α-syn. In our hands the A30P α-syn displayed a lag phase of approximately 1 day by ThT fluorescence (Figure 1 triangles), and fibrils were detectable at day 2 by EM (Figure 2). The A30P α-syn formed amyloid material at an increased rate when compared to WT α-syn. By gel filtration A30P displays a minor peak at 8.8 mL at day 0 which would indicate the rapid formation of an oligomeric species (Supporting Information Figure 1). Rapid oligomerization leading to amyloid fibril formation has been previously reported for β2 microglobulin where tetramers and up to octamers were observed within 1 min following the onset of amyloid formation (*30*). The A30P α-syn was similar to both WT and A53T α-syn and generated ~10−20 nm spherical aggregates during the lag phase (days 0 and 1) which then converted into fibrils from day 2 onward. However, smaller aggregates were visible until day 4. There have been previous reports of mutant α-syn showing an increase in oligomerization but not fibrillization (*15*). The increase in the rate of fibrillization by A30P α-syn, as compared to WT α-syn, in our study may reflect the higher protein concentration and sample agitation that we used, since lower protein concentrations can favor the formation of oligomeric or protofibrilar end products (*31*). As will be demonstrated later, A30P appears to populate a tight binding intermediate at very early time points which may reflect the increased rate of oligomerization associated with this mutation (*9*).

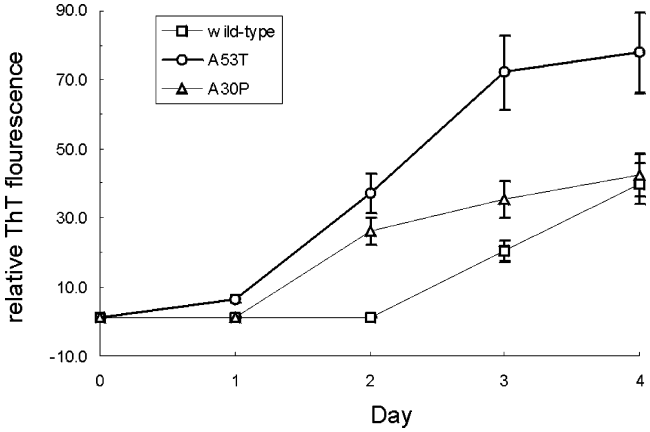

FIGURE 1: Amyloid formation by WT (squares), A53T (circles), and A30P (triangle) α-syn as a function of time as monitored by ThT fluorescence. Protein was incubated at 200 μM, 37 °C, with agitation at 200 rpm for 4 days.

SPR Analysis of WT and Mutant α-Syn Binding to a Lipid Membrane. Both *in vitro* and *in vivo* WT and A53T α-syn can bind to membranes containing acidic phospholipids with a strong preference for phosphatidylserine (*32*−*35*), whereas A30P α-syn displays weaker binding (*2*, *3*, *17*, *18*, *36*). In order to investigate the relationship between the lipid binding, as a function of α-syn aggregation, the apparent protein/lipid dissociation constants (K_{app}) were calculated by SPR. To obtain dissociation constants the α-syn was incubated at 37 °C with agitation over a period of 4 days. A lipid membrane composed of POPC/POPS was laid down onto a L1 BiaCore sensor chip. Lipid was injected until the surface of the chip was fully saturated, i.e., no further increase in RU was observed (Supporting Information Figure 2). In order to prevent nonspecific binding, 4 × 50 μL aliquots of 10 μM BSA at 1 mg/mL were injected over the surface of the chip to block any areas not covered by lipid prior to the injection α-syn. Protein samples, ranging in concentration from 200 to 1.5 μM (~3.2 mg/mL to 0.02 mg/mL), were injected over the captured lipid surface. The injection times were sufficient to allow equilibrium to be reached (Figure

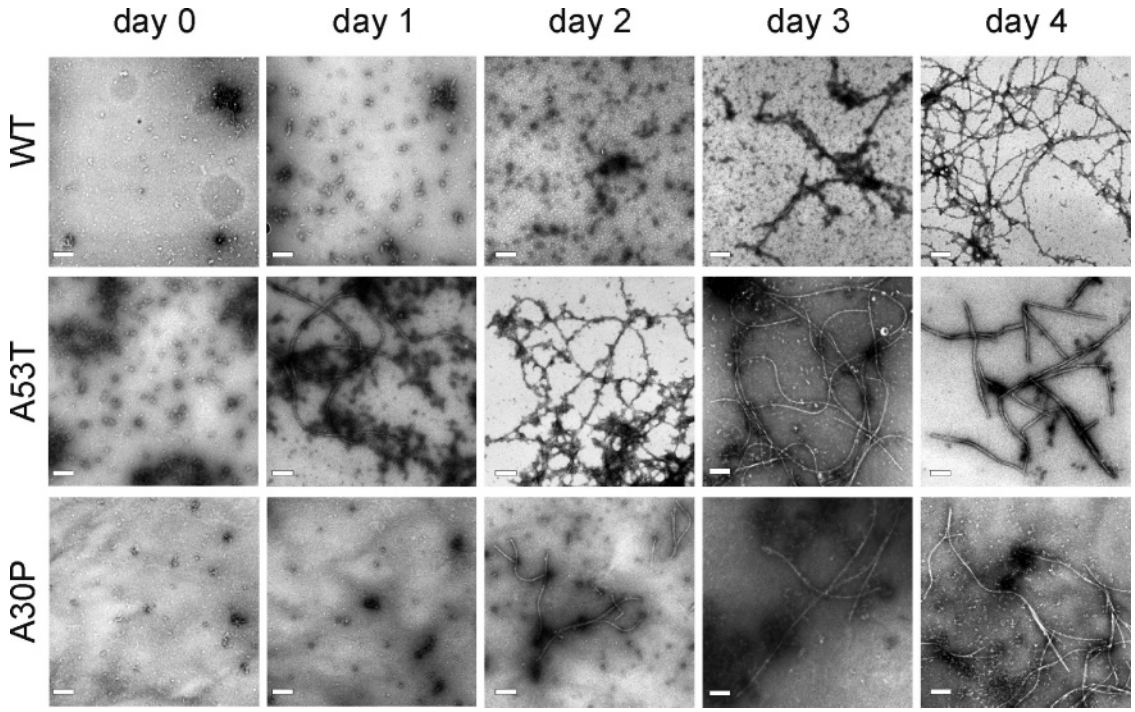

FIGURE 2: Negative stain electron microscopy images of WT, A53T, and A30P α-syn. The protein samples were incubated at 200 μM, 37 °C, with agitation at 200 rpm for 4 days. Scale bar represents 100 nm.

3). The lipid was regenerated by a short injection of 10 mM sodium hydroxide, 100 mM NaCl to remove-bound α-syn. All experiments were carried out at 37 °C. Both aged and unaged WT, A30P, and A53T α-syn-bound reversibly to the lipid membrane and the response signal returned to baseline after a >60 min wash period. To limit any bulk shift effects each sample was prepared in the same running buffer used in the SPR experiments. Sensorgrams were corrected by normalizing the resonance units (RU) values to 0 immediately before injection and by subtracting a buffer blank. In order to obtain apparent dissociation constants the concentration of the protein/lipid complex was measured directly as the steady-state response (R_{eq}) between 340 and 360 s at which point there was little change in RU (Figure 3). α-syn can bind to zwitterionic lipids such as POPC (*34*, *35*) and preliminary experiments by SPR confirmed this observation. Hence, the immobilization chemistry employed here means that an appropriate reference surface cannot be found that would allow the bulk shift to be effectively removed. Because of the fast on rates and long off rates, direct fitting of the sensorgrams was not practical. Scatchard analysis of WT and mutant α-syn were nonlinear, indicating a two-state system and this was interpreted as multiple high- and low-affinity binding interactions (*37*, *38*). On this basis the following model was used to describe the observed data.

$$R_{eq}(\text{est.}) \sim \frac{R_{max}1[A]_o}{K_{app}1 + [A]_o} + \frac{R_{max}2[A]_o}{K_{app}2 + [A]_o}$$

Because of the continual flow of the protein over the sensor chip, the concentration of free protein is equal to the bulk protein concentration $[A]_o$. The steady-state binding level, $R_{eq,}$ can be described by the equation were R_{max} is the initial concentration of ligand, i.e., the maximum protein binding capacity and K_{app} is the apparent dissociation constant for this system. Dissociation constants were established by fitting binding curves to the above model and are reported as Scatchard plots ($R_{eq}/[A]_o$ vs R_{eq}) (Figure 4). The high affinity dissociation constants ($K_{app}1$) were in the micromolar range. The low affinity dissociation constants ($K_{app}2$) were >300 μM in all cases. Since the low affinity $K_{app}2$ was not fully covered by the concentration range used in this experiment, in addition to the heterogeneous nature of the protein at the later time points, the dissociation constants represent qualitative estimations. The weak $K_{app}2$ most likely corresponds to a nonspecific change in the refractive index (bulk shift) as the protein sample passes over the surface of the immobilized lipid.

Apparent dissociation constants for WT and mutant α-syn were obtained through the lag phase period of fibril growth and are shown in Figure 4 and summarized in Table 1. WT α-syn displayed a lag phase of 2 days when incubated at 200 μM with agitation (Figure 1). At day 0 the SPR analysis revealed a $K_{app}1 \sim 13.4\ \mu M \pm 4.6$ corresponding to the binding of α-syn to the lipid bilayer plus a nonspecific binding phase $K_{app}2$ of >300 μM. At day 1 a stronger $K_{app}1 \sim 0.3\ \mu M \pm 0.7$ was observed along with an increase in the amount of protein-bound RU = 1400 (Figure 3 and 4). This dissociation constant decreased to 7.7 μM ± 2.7 at day 2 with a corresponding loss in the amount of bound protein. The A53T α-syn, with its significantly reduced lag phase of less than 1 day, displayed a higher affinity $K_{app}1 \sim 0.7\ \mu M \pm 0.3$ at day 0. At day 1 the dissociation constant decreased to $K_{app}1 \sim 8.8\ \mu M \pm 4.0$. These results indicate that both WT and A53T generated an apparent high affinity binding species during the lag phase of fibril growth and the appearance of the high affinity binding species corresponded to their relative aggregation rates. In contrast, A30P α-syn displayed a dissociation constant of $K_{app}1 \sim 5.0\ \mu M \pm 1.3$ at day 0 and a single weak $K_{app} > 300\ \mu M$ is observed at day 1. It is most likely that upon aging the A30P α-syn loses its ability to bind to the lipid membrane and the observed

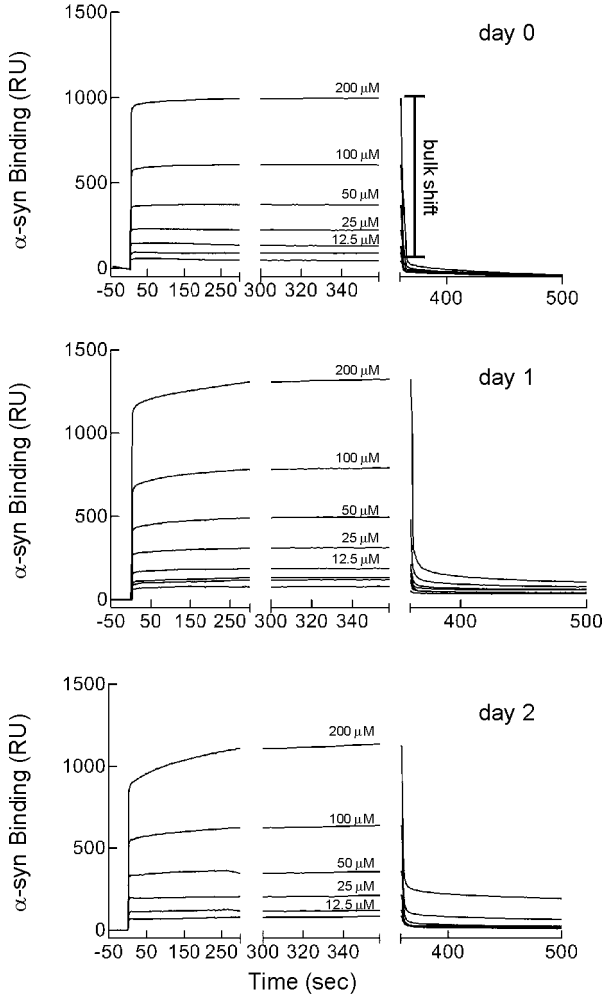

FIGURE 3: Sensorgrams demonstrating the binding of WT α-syn at days 0, 1, and 2 to a POPC/POPS lipid membrane. WT α-syn was prepared at 200 μM and allowed to age at 37 °C with agitation. Samples were then serially diluted over the concentration range 200−1.5 μM and injected for 360 s, after which point the membrane was washed with running buffer to allow dissociation. Equilibrium data were collected from 340 to 360 s, at which point there was little to no change in RU. The break in the sensorgram represents a change in scale. An increase in the concentration of WT α-syn-bound binding to the lipid membrane can be observed at day 1 as in increase in steady-state RU as compared to days 0 and 2.

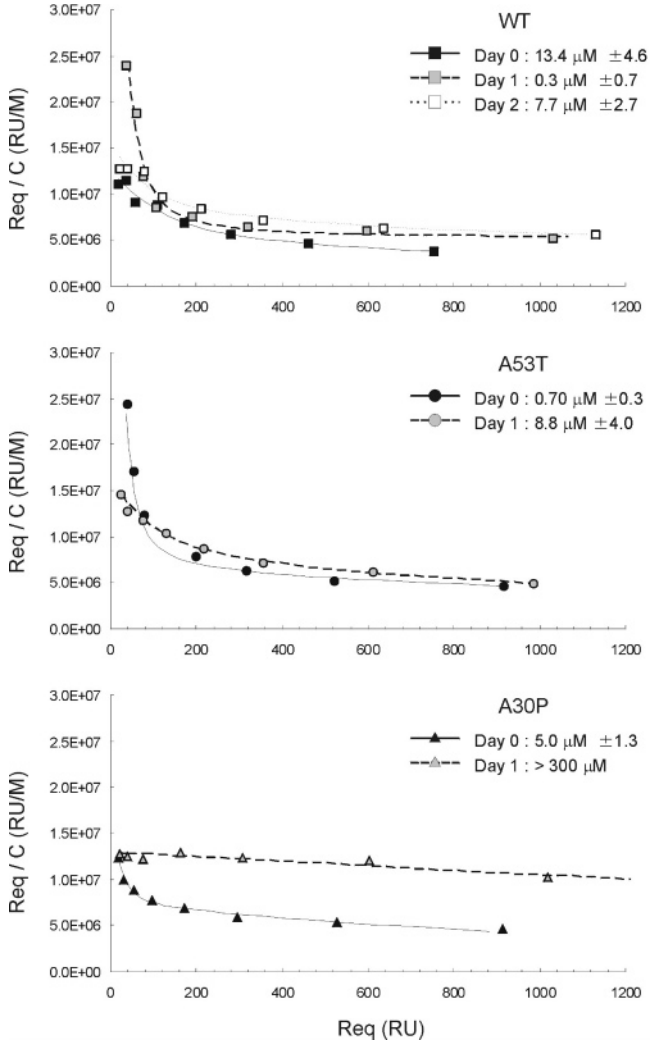

FIGURE 4: Scatchard plot analysis of WT α-syn (squares), A53T (circles), and A30P (triangles) binding to POPC/POPS lipid membranes. Binding data was obtained over a 200−1.5 μM concentration, and the RU signal at equilibrium was recorded (R_{eq}). This data was then used to construct Scatchard plots from which the apparent protein/lipid dissociation constants (K_{app}) were calculated via a two state model. The values for $K_{app}1$ are indicated. In all cases a $K_{app}2$ was greater than 300 μM and has been omitted for clarity. Samples were incubated for 0 (black), 1 (gray), and 2 (white) days at 37 °C with agitation at 200 rpm

interaction (K_{app} > 300 μM) only reflects the change in refractive index due to the protein passing over the chip surface. These results suggest that A30P α-syn generates a species with similar binding properties to WT and A53T α-syn during the early stages of fibril formation. Yet upon further aging the A30P α-syn mutant then appears unable to bind to the lipid membrane. SPR does not distinguish between the binding of a single fibril containing many protein subunits and the equivalent number of subunits binding individually. Hence, while it was not possible to calculate apparent protein/lipid dissociation constants for fibrillar material because of the large and heterogeneous nature of the aggregates it was possible to detect binding.

To further define the formation of this high affinity lipid binding species, WT, A53T, and A30P α-syn were incubated at 37 °C without agitation in order to slow the rate of fibril formation. At day 0 the samples were kept on ice until injection on to the chip in order to minimize aggregation. The dissociation constants of the unagitated sample were then acquired by SPR (Table 1). At day 0 without agitation WT α-syn displays a $K_{app}1 \sim 9.4$ μM ± 2.8. After 1 day of incubation the dissociation constant was 10.9 μM ± 5.0 and after day 2 a $K_{app}1 \sim 1.5$ μM ± 1.4 was observed corresponding to the formation of the high affinity binding intermediate. In contrast, the agitated sample formed the high affinity binding species at day 1. The A53T α-syn displayed a similar pattern of binding with a $K_{app}1 \sim 2.8$ μM ± 0.7 at day 0 increasing to 0.3 μM ± 0.7 at day 1 and then decreasing to 2.2 μM ± 1.8 at day 2. The A30P α-syn, however, behaved in a similar manner to the agitated sample displaying at day 0 an $K_{app}1 \sim 6.7$ μM ± 1.8 that decreased to >300 μM by day 1. The binding of A30P at day 0 may reflect this mutant's increased tendency to form oligomers and protofibrils (*9*), and it is possible that A30P α-syn can rapidly form oligomers before the start of the experiment as indicated by the gel filtration results. These results would suggest that the formation of the high affinity binding

Table 1: Apparent Dissociation Constants for WT, A53T, and A30P α-syn with a POPC/POPS Lipid Membrane[a]

	day 0, μM	day 1, μM	day 2, μM
WT	13.4 ± 4.6	0.3 ± 0.7	7.7 ± 2.7
A53T	0.7 ± 0.3	8.8 ± 4.0	—[b]
A30P	5.0 ± 1.3	>300	—[b]
	no agitation		
WT	9.4 ± 2.8	10.9 ± 5.0	1.5 ± 1.4
A53T	2.8 ± 0.7	0.3 ± 0.7	2.2 ± 1.8
A30P	6.7 ± 1.8	>300	>300

[a] Binding data was obtained over a range of concentrations (200−1.5 μM) and the RU signal at equilibrium was recorded (R_{eq}). This data was then used to construct Scatchard plots from which the apparent protein/lipid dissociation constants (K_{app}) were calculated *via* a two state model. The values for $K_{app}1$ are indicated. In all cases a $K_{app}2$ was greater than 300 μM and has been omitted for clarity. Samples were incubated for 0 to 4 days at 37 °C with or without agitation at 200 rpm. [b] Time points at which it was not possible to gain data because of the presence of fibrillar material.

intermediate, at least in the case of WT and A53T, is dependent on the rate of aggregation and that slowing fibril growth delays the formation of these species.

WT α-syn Binding to LUV. In vivo α-syn is known to bind to both curved synaptic vesicles and lipid rafts (*23*, *33*, *34*, *39*). We have demonstrated by SPR that WT α-syn will bind to a synthetic lipid membrane with a $K_{app}1 \sim 13.4$ μM ± 4.6. Since the SPR technique described above results in the formation of a flat lipid bilayer on the surface of the sensor chip, we repeated the day 0 binding experiment using circular dichroism (CD) with 100 nm LUVs to ascertain if curvature of the lipid membrane affects the protein lipid dissociation constant. We assessed protein/LUV binding by monitoring the observable conformational change from a random coil to an α-helical structure following lipid binding at 222 nm (*25*). It is not possible to monitor the change in dissociation constants due to aggregation with this method, as the aggregated material undergoes an altered conformational change upon lipid binding (see below). All interactions of the peptide with the lipid vesicles are assumed to be equivalent and occupancy independent. The observed Scatchard plot was linear suggesting the presence of a single binding event (*37*) (Supporting Information Figure 3), and the dissociation constant was 2.3 μM ± 1. The lack of a second phase in this experiment reflects the manner in which it was performed. SPR utilizes a constant flow of protein over the surface of a bound membrane, and it monitors interactions via the change in refractive index, resulting in a nonspecific bulk-shift as described above. In contrast, the CD experiments monitor the change in structure upon binding, and hence no such nonspecific binding events are observed. The data would suggest that unaged WT α-syn has a higher affinity for curved lipid membranes as compared to a flat membrane.

Perturbation of the Lipid Membrane upon α-syn Binding. To determine the nature of binding and the ability of WT and mutant α-syn to perturb the lipid membrane upon binding, the anisotropy of DPH (diphenyl-1,3,5-hexatriene) in a lipid environment was monitored. DPH intercalates axially within the acyl-chain region of the lipid bilayer, and its anisotropy indicates the fluidity of this hydrophobic environment (*40*). When WT, A30P, and A53T α-syn were incubated with LUV during their respective lag phases there were no significant changes in the fluidity of the acyl-chain region (Figure 5). However, upon the formation of ThT reactive material (Figure 1) there was perturbation of the acyl-chain region as seen by the decrease in fluidity (Figure 5). Therefore, the high affinity binding species observed by SPR on day 0 for A53T and A30P and on day 1 for WT does not significantly alter the fluidity of the acyl-chain region of the lipid bilayer. However, the formation of ThT reactive α-syn induces changes in fluidity of the lipid acyl-chain region.

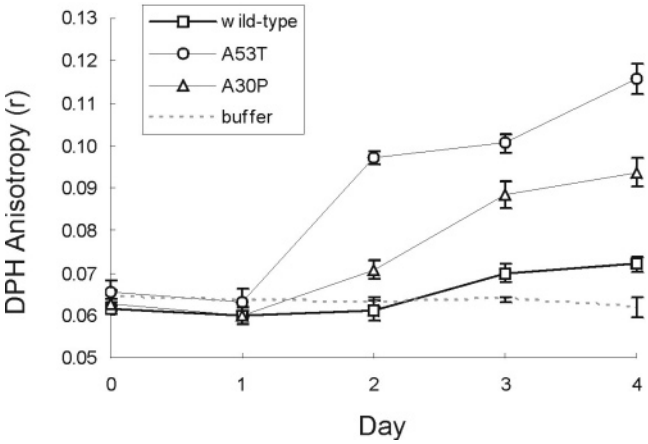

FIGURE 5: The effect of aggregating α-syn (squares), A53T (circles), and A30P (triangles) on the fluidity of the acyl-chain region of LUV. Steady-state anisotropy (*r*) of the fluorescent probe DPH in synthetic LUV (POPC/POPS).

Secondary Structure Transitions Observed on Lipid Binding. α-syn binds to both synaptic vesicles and lipid rafts (*23*, *33*, *34*, *39*) and undergoes a structural change from a random coil toward a more α-helical structure (*2*, *25*). To investigate how this lipid-induced structural change is affected by aggregation, WT, A30P, and A53T α-syn were aggregated in the absence of lipid, and then far-UV CD spectra were acquired before and immediately after the addition of POPC/POPS LUVs at 37 °C (Figure 6). Insoluble material was removed from the samples prior to addition to LUVs *via* centrifugation. The concentration of the resulting supernatant was determined and used to normalize the CD spectra to mean residue elliptically. At no point was the α-syn aggregated in the presence of LUVs. WT α-syn at day 0 displayed a characteristic spectrum for an unstructured protein with a strong negative peak at 200 nm (Figure 6a). Upon the formation of ThT reactive material, at days 3 and 4, there was an increase in the signal at ∼216−218 nm and a decrease in the 200 nm signal, consistent with an increase in β-sheet content (*15*). As expected, unaged WT α-syn upon binding to the negatively charged lipid membrane underwent a shift from random-coil to a more α-helical structure with strong double minima peaks at 208 and 222 nm (Figure 6b). Aging for only 1 day, and coinciding with the formation of the high affinity binding intermediate, enhanced the ability of the remaining soluble WT α-syn to undergo a structural transition into an α-helical species. There was a marked increase in the intensity of the 208 and 222 nm signals, resulting in a higher proportion of α-helical content increasing from 20 to 25% (Table 2). The concentration of the protein in the supernatant was used to normalize the CD spectra, and this indicated that the alteration in spectral shape was due to a change in the conformation of the bound α-syn

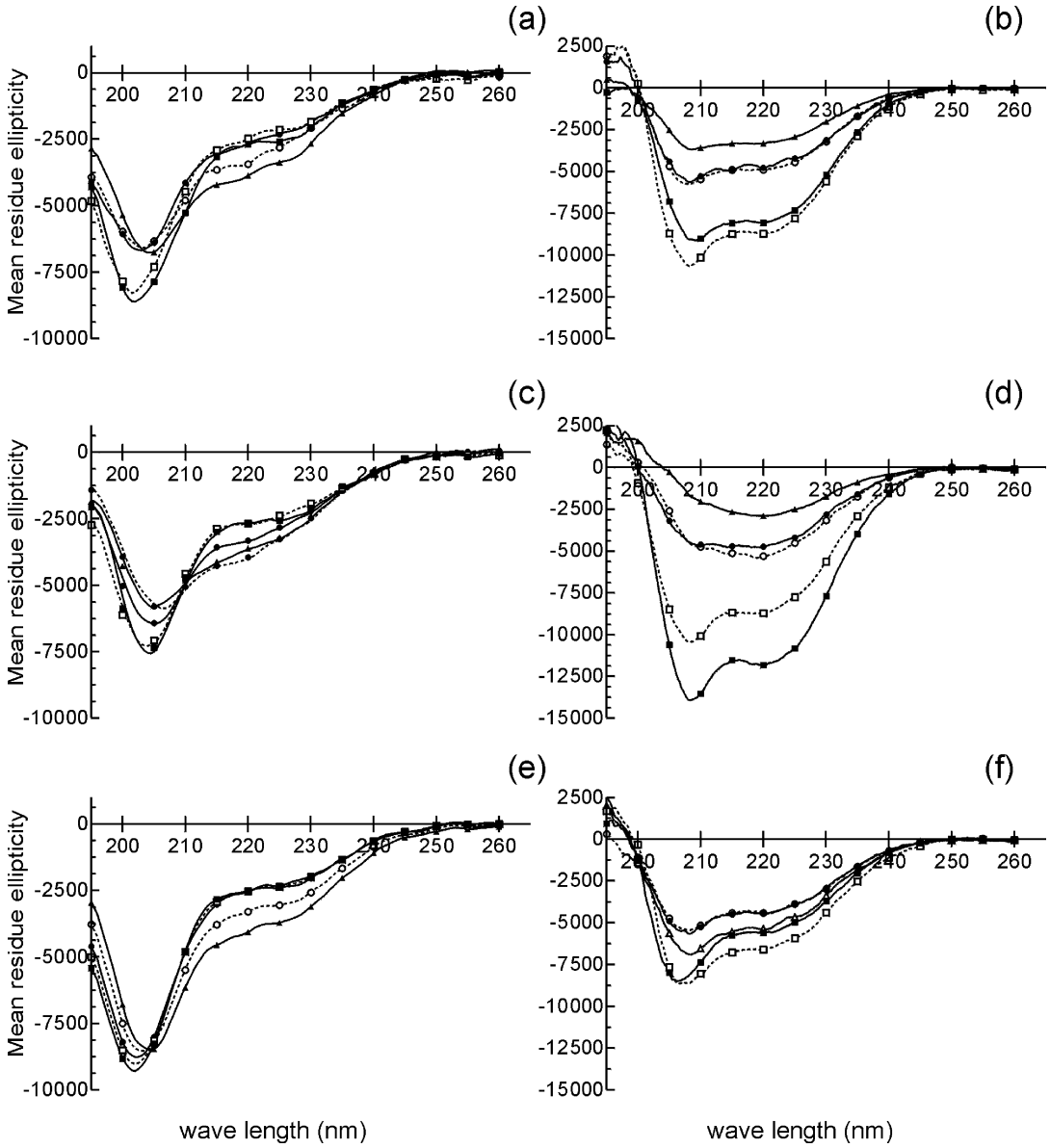

FIGURE 6: Far UV CD spectra of WT α-syn and its mutants (15 μM) in the presence and absence of LUV (POPC/POPS) (4 mM) at 37 °C. Protein was allowed to aggregate for the given time before insoluble material was removed via centrifugation, and the supernatant was mixed with LUV (a) WT α-syn, (b) WT α-syn + LUV, (c) A53T (d) A53T + LUV, (e) A30P, (f) A30P + LUV. Shape represents the number of days of incubation: 0 day, closed square; 1 day, open square; 2 days, closed circle; 3 days, open circle; 4 days, closed triangle.

Table 2: % α-Helix as a Function of Aggregation of α-syn and Its Mutants[a]

% α-helix	WT	A30P	A53T
day 0	20	19	42
day 1	25	21	23
day 2	16	12	10
day 3	12	11	10
day 3	8	13	6

[a] Data were analyzed using the CDSSTR algorithm from the Dicroweb website, http://public-1.cryst.bbk.ac.uk/cdweb/html. The CD spectra were obtained using a Jasco 815 spectropolarimeter at 37 °C. Far-UV CD spectra were collected from 185 to 260 nm using a cuvette with a 0.1 cm path length. The baseline acquired in the absence of peptide was subtracted.

and not due to a loss of protein from the solution. Further aging increased the formation of ThT reactive material, which resulted in a decrease in the concentration of soluble α-syn and a decrease in the protein's ability to undergo a structural change toward an α-helical structure upon lipid binding.

In this study the A53T α-syn forms amyloid material more rapidly than WT α-syn (Figures 1 and 2), and this observation is supported by the far UV CD spectra (Figure 6c). The negative peak at 216−218 nm observed for the WT α-syn at days 3 and 4 is clearly visible at day 2 in the case of A53T. Upon further aging the signal increased, and there was little change in the spectra between days 3 and 4. Of particular interest is that the far-UV CD spectra of WT α-syn at day 4 and A53T α-syn at day 2 are virtually identical. At these time points both proteins display a similar ThT signal (Figure 1) and EM morphology (Figure 2). In the presence of lipid membranes the A53T α-syn also underwent a conformational change into an α-helical structure with negative signals at 208 and 222 nm. However, at day 0 soluble A53T was able to form a lipid-bound species with an α-helical content of 42% (Table 2), indicating that lipid-bound A53T α-syn contained a greater amount of α-helical structure than WT α-syn, and this coincided with the

formation of the tight membrane binding species. Akin to WT α-syn, aging A53T α-syn decreased its ability to convert into α-helix upon lipid binding as seen by decreased signals at both 208 and 222 nm and a loss of total α-helical content. Un-aged A30P α-syn displays weaker α-helical signal in the presence of POPC/POPS LUV; however, the total helical content was 19%. Aging A30P α-syn caused the total helical content to decrease in intensity as the protein converted into ThT reactive material.

DISCUSSION

In this study we have utilized SPR to investigate the interaction of α-syn with negatively charged lipid bilayers as a function of protein aggregation. Using a two-state model as a function of protein aggregation, we determined apparent dissociation constants for WT α-syn and the A53T and A30P mutants. The WT α-syn binds to an immobilized lipid bilayer with a $K_{app}1 \sim 13.4\ \mu M \pm 4.6$ and undergoes a structural change toward α-helix. After 1 day of incubation at 37 °C, with agitation, the WT α-syn $K_{app}1$ increased almost 100-fold to $0.3\ \mu M \pm 0.7$ with a concurrent increase in bound material. The remaining soluble protein's ability to undergo a structural transition to α-helix was increased from 20 to 25%, indicating that a conformational change had occurred. After 2 days of incubation the $K_{app}1$ decreases to $7.7\ \mu M \pm 2.7$, and the ability of WT α-syn to form a lipid-associated α-helix is further diminished. A53T α-syn, which aggregated more readily than the WT protein, generates a high affinity binding species at day 0 ($K_{app}1 \sim 0.7\ \mu M \pm 0.3$) with a lipid-bound species displaying 42% α-helix. This was followed by a decrease in $K_{app}1$ to $8.8\ \mu M \pm 4.0$ at day 1, concurrent with the formation of a small amount of fibrillar material as demonstrated by ThT fluorescence and EM and a loss in the proteins ability to form helical structures. Agitation is known to increase the rate of fibril formation; thus, when WT and A53T α-syn were incubated without agitation, the high affinity binding intermediate appeared at day 2 instead of day 1 for WT α-syn and at day 1 instead of day 0 for A53T. This suggested that the high affinity binding intermediate arises as a function of fibril formation. Thus, WT and A53T α-syn generate high affinity lipid binding species during the lag phase of fibril formation, displaying an increase in the ability to form an α-helical structure at least in the case of the WT protein. In addition, DPH fluorescence anisotropy measurements indicated that fibril binding to the membrane results in the perturbation of the acyl-chain region of the lipid bilayer, resulting in a decrease in fluidity; similar results have been reported by Zhu et al. (*23*). Kamp et al. demonstrated that α-syn incubated with SUV, composed of a POPC/POPG mixture at 21 °C, induced an increase in anisotropy of DPH upon lipid binding by raising the transition temperature of the vesicles which in turn heals the packing defects in the highly curved membranes (*41*). We however did not see any change in DPH anisotropy at similar protein/lipid ratios upon lipid binding of unaged α-syn. Presumably, this is because of the higher temperature (37 °C) at which our experiments where carried out and the alternate use of LUV's. In addition Kamp et al. reported a ~1.5 nm blue shift in laurdan fluorescence at 30 °C using POPC/POPG indicating a tighter lipid packing of the bilayer interface (*41*). A30P α-syn, unlike WT and A53T α-syn, has been reported to have a weak affinity for lipid membranes (*16*, *17*, *19*, *21*, *22*); however, we identified that A30P α-syn generates a transient lipid binding intermediate at day 0. In comparison to WT α-syn, both A30P and A53T α-syn display accelerated formation of oligomers and protofibirls (*9*, *15*). Furthermore, the weak binding of A30P α-syn to lipid membranes corresponds to a dimeric species (*17*). Because of our experiment design there is an unavoidable delay before the first injection occurs, and it is possible that during this time period the A30P α-syn has already partially aggregated, forming the binding species observed by SPR. However, upon further incubation this binding affinity is lost, as fibrils are formed and only a single weak species with a $K_{app} > 300\ \mu M$ is observed. The formation of partially aggregated or oligomeric species will be concentration dependent and at lower initial concentrations the unaggregated nonlipid binding A30P α-syn monomer would be the dominant species. From our results A30P α-syn appears to form a partially aggregated, or conformationally altered, high affinity binding species at close to $t = 0$, which then extends to form fibrils and a range of small aggregates, presumably leaving only the monomer in solution, which is incapable of lipid binding. It has been demonstrated that both A53T and A30P at high protein concentrations (200 μM/~3 mg/mL) have an increased propensity for aggregation and oligomer formation at the early time points with an increased β-sheet content of 1.54 (A30P) and 1.85 times (A53T) greater that that of the WT protein being reported *via* FTIR (*42*). This initial increase in oligomer content may explain the increase in binding affinity and rapid fibril formation of both mutants at the concentrations used.

The formation of the high affinity binding species observed here corresponded to the presence of the spherical aggregates observed by EM. Lashuel et al. (*43*) and Volles et al. (*44*) have both previously observed the formation of spherical aggregates or protofibirls with a similar size distribution to that observed here. However, Lashuel et al. (*43*) also observed the formation of annular protofibrils with diameters ~11 nm. Volles et al. (*44*) demonstrated that protofibrillar WT α-syn binds to negatively charged 100% egg-derived phosphatidylglycerol membranes with similar estimated affinities in the nanomolar range to those reported here. Furthermore, α-syn can bind to oleic acid with a K_d of 12.5 μM (*45*). However, in contrast to our data, experiments using intrinsic fluorescence with unaged α-syn binding to either a 100% POPS or 100% POPC LUV yielded $K_d \sim 1.5\ \mu M \pm 0.32$ and $1.6\ \mu M \pm 0.5$, respectively (*34*). These differences in the affinity of α-syn binding to lipid at day 0 as monitored by intrinsic fluorescence (*34*) and here by SPR presumably reflect the preference of α-syn to bind with a higher affinity to the more curved lipid membranes of the LUV (*34*) as compared to the flat lipid surface on the SPR chip. To confirm this explanation, we measured the binding of WT α-syn to POPC/POPS LUV at day 0 by CD and obtained a single dissociation constant of $2.3\ \mu M \pm 1$. This observation reflects the preferential *in vivo* binding of α-syn to synaptic vesicles (*17*, *21*−*23*) which have a mean diameter of 39.7 ± 6.6 nm (*46*). α-syn binding is known to be accompanied by a random coil−helix transition that leads to an increase in chain melting temperatures and an enhanced cooperativity of the phase transition attributed to defective healing in the curved vesicle membrane (*41*). This suggests a possible role for α-syn lipid binding *in vivo* as a stabilizer of synaptic

vesicles (*41*). α-syn can also form high-molecular weight protein/lipid complexes with free fatty acids which populate a range of oligomeric species as observed *via* western blot and NMR (*47*). However dimers and high order oligomers were not observed in lipid-free solutions (*47*), and the WT samples in this study were unaged prior to the addition of lipid. Our results would indicate that the high affinity species only appears after a period of incubation. On the basis of these results, it was concluded that α-syn is not a member of the intercellular fatty acid binding protein family (*47*). Disruption of lipid particles by α-syn was observed at 1:1 molar ratios upon vortexing (*47*), and high concentrations of α-syn lipid membranes can be dissolved *via* a detergent-like mechanism (*48*). Therefore, careful regulation of α-syn expression and localization may be required *in vivo* as excessive levels or mislocalization of the protein may lead to the formation of oligomers with high affinity lipid binding activity that is capable of disrupting cellular membranes.

The formation of the α-syn high affinity binding species observed here appears to be dependent on the rate of aggregation, suggesting that it is an oligomeric intermediate populated during the amyloid formation phase. Using a similar system, there was an increase in the affinity of transthyretin binding during amyloid formation to a lipid membrane as measured by SPR (*49*). Tryptophan mutants of α-syn showed that a conformational change, tending toward a β-sheet rich oligomer, takes place near the end of the lag phase (*50*, *51*). C-Terminally truncated α-syn can bind with an increased affinity to lipid membranes and up to 30−40% of lipid-bound WT, and truncated α-syn has a β-sheet structure (*36*). Moreover, the generation of a dimeric species is a critical first step in aggregation (*52*), and α-syn dimers are present *in vivo* and can strongly associate with lipid vesicles (*17*, *24*). Soluble amyloid oligomers from different proteins are capable of permeating lipid bilayers (*53*). Yeast toxicity by α-syn has been observed and hypothesized to be caused by α-syn binding directly to membranes at levels sufficient to nonspecifically disrupt homeostasis (*54*). Furthermore, it was concluded that non-fibrillar α-syn mediates this toxicity and nontoxic variants have decreased membrane-binding ability (*54*). In this context oligomeric α-syn is known to be toxic (*55*), and membrane-bound α-syn has been associated with oxidative stress (*56*). Therefore, it is feasible that the high affinity binding species observed here by SPR may correspond to a toxic species responsible, in part, for PD.

ACKNOWLEDGMENT

We thank Dr. Edouard Nice of the Ludwig Institute for Cancer Research Melbourne, Australia, for critically reading the manuscript. Anna Friedhuber, Department of Pathology, The University of Melbourne, for assistance with the electron microscopy.

SUPPORTING INFORMATION AVAILABLE

Figure S1: Gel filtration of WT α-syn, A53T, and A30P. Figure S2: Sensorgrams demonstrating the binding of POPC/POPS to the L1 BiaCore sensor chip. Figure S3: Binding curve for WT α-syn binding to POPC/POPS LUV derived from CD data. This material is available free of charge via the Internet at http://pubs.acs.org.

REFERENCES

1. Dauer, W., and Przedborski, S. (2003) Parkinson's disease: mechanisms and models, *Neuron 39*, 889−909.
2. Eliezer, D., Kutluay, E., Bussell, R., Jr., and Browne, G. (2001) Conformational properties of alpha-synuclein in its free and lipid-associated states, *J. Mol. Biol. 307*, 1061−1073.
3. Davidson, W. S., Jonas, A., Clayton, D. F., and George, J. M. (1998) Stabilization of alpha-synuclein secondary structure upon binding to synthetic membranes, *J. Biol. Chem. 273*, 9443−9449.
4. Uversky, V. N., Li, J., and Fink, A., L. (2001) Metal-triggered structural transformations, aggregation, and fibrillation of human α-synuclein, *J. Biol. Chem. 276*, 44284−44296.
5. Weinreb, P. H., Zhen, W., Poon, A. W., Conway, K. A., and Lansbury, P. T., Jr. (1996) NACP, a protein implicated in Alzheimer's disease and learning, is natively unfolded, *Biochemistry 35*, 13709−13715.
6. Der-Sarkissian, A., Jao, C. C., Chen, J., and Langen, R. (2003) Structural organization of alpha-synuclein fibrils studied by site-directed spin labeling, *J. Biol. Chem. 278*, 37530−37535.
7. Wood, S. J., Wypych, J., Steavenson, S., Louis, J. C., Citron, M., and Biere, A. L. (1999) alpha-synuclein fibrillogenesis is nucleation-dependent. Implications for the pathogenesis of Parkinson's disease, *J. Biol. Chem. 274*, 19509−19512.
8. Morris, H. R. (2005) Genetics of Parkinson's disease, *Ann. Med. 37*, 86−96.
9. Conway, K. A., Lee, S. J., Rochet, J. C., Ding, T. T., Harper, J. D., Williamson, R. E., and Lansbury, P. T., Jr. (2000) Accelerated oligomerization by Parkinson's disease linked alpha-synuclein mutants, *Ann. N. Y. Acad. Sci. 920*, 42−45.
10. Conway, K. A., Harper, J. D., and Lansbury, P. T., Jr. (2000) Fibrils formed in vitro from α-synuclein and two mutant forms linked to Parkinson's disease are typical amyloid, *Biochemistry. 39*, 2552−25563.
11. Greenbaum, E. A., Graves, C. L., Mishizen-Eberz, A. J., Lupoli, M. A., Lynch, D. R., Englander, S. W., Axelsen, P. H., and Giasson, B. I. (2005) The E46K mutation in alpha-synuclein increases amyloid fibril formation, *J. Biol. Chem. 280*, 7800−7807.
12. Conway, K. A., Harper, J. D., and Lansbury, P. T. (1998) Accelerated in vitro fibril formation by a mutant alpha-synuclein linked to early-onset Parkinson disease, *Nat. Med. 4*, 1318−13120.
13. Tabrizi, S. J., Orth, M., Wilkinson, J. M., Taanman, J. W., Warner, T. T., Cooper, J. M., and Schapira, A. H. (2000) Expression of mutant alpha-synuclein causes increased susceptibility to dopamine toxicity, *Hum. Mol. Genet. 9*, 2683−2689.
14. Narhi, L., Wood, S. J., Steavenson, S., Jiang, Y., Wu, G. M., Anafi, D., Kaufman, S. A., Martin, F., Sitney, K., Denis, P., Louis, J. C., Wypych, J., Biere, A. L., and Citron, M. (1999) Both familial Parkinson's disease mutations accelerate alpha-synuclein aggregation, *J. Biol. Chem. 274*, 9843−9846.
15. Conway, K. A., Lee, S. J., Rochet, J. C., Ding, T. T., Williamson, R. E., and Lansbury, P. T., Jr. (2000) Acceleration of oligomerization, not fibrillization, is a shared property of both alpha-synuclein mutations linked to early-onset Parkinson's disease: implications for pathogenesis and therapy, *Proc. Natl. Acad. Sci. U.S.A. 97*, 571−576.
16. Bussell, R., Jr., and Eliezer, D. (2004) Effects of Parkinson's disease-linked mutations on the structure of lipid-associated alpha-synuclein, *Biochemistry 43*, 4810−4818.
17. Jo, E., Fuller, N., Rand, R. P., St, George-Hyslop, P., and Fraser, P. E. (2002) Defective membrane interactions of familial Parkinson's disease mutant A30P alpha-synuclein, *J. Mol. Biol. 315*, 799−807.
18. Chandra, S., Chen, X., Rizo, J., Jahn, R., and Sudhof, T. C. (2003) A broken alpha-helix in folded alpha -Synuclein, *J. Biol. Chem. 278*, 15313−15318.
19. Perrin, R. J., Woods, W. S., Clayton, D. F., and George, J. M. (2000) Interaction of human alpha-Synuclein and Parkinson's disease variants with phospholipids. Structural analysis using site-directed mutagenesis, *J. Biol. Chem. 275*, 34393−34398.
20. Dixon, C., Mathias, N., Zweig, R. M., Davis, D. A., and Gross, D. S. (2005) Alpha-synuclein targets the plasma membrane via the secretory pathway and induces toxicity in yeast, *Genetics 170*, 47−59.
21. Jensen, P. H., Nielsen, M. S., Jakes, R., Dotti, C. G., and Goedert, M. (1998) Binding of alpha-synuclein to brain vesicles is abolished by familial Parkinson's disease mutation, *J. Biol. Chem. 273*, 26292−26294.

22. Fortin, D. L., Troyer, M. D., Nakamura, K., Kubo, S., Anthony, M. D., and Edwards, R. H. (2004) Lipid rafts mediate the synaptic localization of alpha-synuclein, *J. Neurosci. 24*, 6715−6723.
23. Zhu, M., Li, J., and Fink, A. L. (2003) The association of alpha-synuclein with membranes affects bilayer structure, stability, and fibril formation, *J. Biol. Chem. 278*, 40186−40197.
24. Cole, N. B., Murphy, D. D., Grider, T., Rueter, S., Brasaemle, D., and Nussbaum, R. L. (2002) Lipid droplet binding and oligomerization properties of the Parkinson's disease protein alpha-synuclein, *J. Biol. Chem. 277*, 6344−52.
25. Cappai, R., Leck, S. L., Tew, D. J., Williamson, N. A., Smith, D. P., Galatis, D., Sharples, R. A., Curtain, C. C., Ali, F. E., Cherny, R. A., Culvenor, J. G., Bottomley, S. P., Masters, C. L., Barnham, K. J., and Hill, A. F. (2005) Dopamine promotes alpha-synuclein aggregation into SDS-resistant soluble oligomers via a distinct folding pathway, *FASEB J. 19*, 1377−1379.
26. Whitmore, L., and Wallace, B. A. (2004) DICHROWEB, an online server for protein secondary structure analyses from circular dichroism spectroscopic data, *Nucleic Acids Res. 32*, W668−W673.
27. Lobley, A., Whitmore, L., and Wallace, B. A. (2002) DICHROWEB: an interactive website for the analysis of protein secondary structure from circular dichroism spectra, *Bioinformatics 18*, 211−212.
28. Smith, D. P., and Radford, S. E. (2001) Role of the single disulphide bond of beta(2)-microglobulin in amyloidosis in vitro, *Protein Sci. 10*, 1775−1784.
29. Conway, K. A., Harper, J. D., and Lansbury, P. T., Jr. (2000) Fibrils formed in vitro from α-synuclein and two mutant forms linked to Parkinson's disease are typical amyloid, *Biochemistry 39*, 2552−2563.
30. Smith, A. M., Jahn, T. R., Ashcroft, A. E., and Radford, S. E. (2006) Direct observation of oligomeric species formed in the early stages of amyloid fibril formation using electrospray ionisation mass spectrometry, *J. Mol. Biol. 364*, 9−19.
31. Li, J., Uversky, V. N., and Fink, A. L. (2001) Effect of familial Parkinson's disease point mutations A30P and A53T on the structural properties, aggregation, and fibrillation of human α-synuclein, *Biochemistry. 40*, 11604−11613.
32. Kubo, S., Nemani, V. M., Chalkley, R. J., Anthony, M. D., Hattori, N., Mizuno, Y., Edwards, R. H., and Fortin, D. L. (2005) A combinatorial code for the interaction of alpha-synuclein with membranes, *J. Biol. Chem. 280*, 31664−31672.
33. Jo, E., McLaurin, J., Yip, C. M., St George-Hyslop, P., and Fraser, P. E. (2000) alpha-Synuclein membrane interactions and lipid specificity, *J. Biol. Chem. 275*, 34328−34334.
34. Narayanan, V., and Scarlata, S. (2001) Membrane binding and self-association of α-synucleins, *Biochemistry 40*, 9927−9934.
35. Rhoades, E., Ramlall, T. F., Webb, W. W., and Eliezer, D. (2006) Quantification of α-synuclein binding to lipid vesicles using fluorescence correlation spectroscopy, *Biophys. J. 90*, 4692−4700.
36. Ramakrishnan, M., Jensen, P. H., and Marsh, D. (2006) Association of α-synuclein and mutants with lipid membranes: spin-label ESR and polarized IR, *Biochemistry 45*, 3386−3395.
37. Dahlquist, F. W. (1978) The meaning of Scatchard and Hill plots, *Methods Enzymol. 48*, 270−299.
38. Roy, M. O., Pugniere, M., Jullien, M., Chopineau, J., and Mani, J. C. (2001) Study of hydrophobic interactions between acylated proteins and phospholipid bilayers using BIACORE, *J. Mol. Recognit. 14*, 72−78.
39. Zhu, M., and Fink, A. L. (2003) Lipid binding inhibits alpha-synuclein fibril formation, *J. Biol. Chem. 278*, 16873−1687.
40. Müller, W. E., Kirsch, C., and Eckert, G. P. (2001) Membrane-disordering effects of *β*-amyloid peptides, *Biochem. Soc. Trans. 29*, 617−623.
41. Kamp, F., and Beyer, K. (2006) Binding of alpha-synuclein affects the lipid packing in bilayers of small vesicles, *J. Biol. Chem. 281*, 9251−9259.
42. Li, J., Uversky, V. N., and Fink, A. L. (2001) Effect of familial Parkinson's disease point mutations A30P and A53T on the structural properties, aggregation, and fibrillation of human α-synuclein, *Biochemistry 40*, 11604−11613.
43. Lashuel, H. A., Petre, B. M., Wall, J., Simon, M., Nowak, R. J., Walz, T., and Lansbury, P. T., Jr. (2002) Alpha-synuclein, especially the Parkinson's disease-associated mutants, forms pore-like annular and tubular protofibrils, *J. Mol. Biol. 322*, 1089−1102.
44. Volles, M. J., Lee, S. J., Rochet, J. C., Shtilerman, M. D., Ding, T. T., Kessler, J. C., and Lansbury, P. T., Jr. (2001) Vesicle permeabilization by protofibrillar α-synuclein: implications for the pathogenesis and treatment of Parkinson's disease, *Biochemistry 40*, 7812−7819.
45. Sharon, R., Goldberg, M. S., Bar-Josef, I., Betensky, R. A., Shen, J., and Selkoe, D. J. (2001) alpha-Synuclein occurs in lipid-rich high molecular weight complexes, binds fatty acids, and shows homology to the fatty acid-binding proteins, *Proc. Natl. Acad. Sci. U.S.A. 98*, 9110−9115.
46. Zhang, B., Koh, Y. H., Beckstead, R. B., Budnik, V., Ganetzky, B., and Bellen, H. J. (1998) Synaptic vesicle size and number are regulated by a clathrin adaptor protein required for endocytosis, *Neuron 21*, 1465−1475.
47. Lucke, C., Gantz, D. L., Klimtchuk, E., and Hamilton, J. A. (2006) Interactions between fatty acids and alpha-synuclein, *J. Lipid Res. 47*, 1714−1724.
48. Volles, M. J., and Lansbury, P. T., Jr. (2002) Vesicle permeabilization by protofibrillar α-synuclein is sensitive to Parkinson's disease-linked mutations and occurs by a pore-like mechanism, *Biochemistry 41*, 4595−4602.
49. Hou, X., Richardson, S. J., Aguilar, M. I., and Small, D. H. (2005) Binding of amyloidogenic transthyretin to the plasma membrane alters membrane fluidity and induces neurotoxicity, *Biochemistry 44*, 11618−11627.
50. Kaylor, J., Bodner, N., Edridge, S., Yamin, G., Hong, D. P., and Fink, A. L. (2005) Characterization of oligomeric intermediates in alpha-synuclein fibrillation: FRET studies of Y125W/Y133F/Y136F alpha-synuclein, *J. Mol. Biol. 353*, 357−372.
51. Dusa, A., Kaylor, J., Edridge, S., Bodner, N., Hong, D. P., and Fink, A. L. (2006) Characterization of Oligomers during α-Synuclein Aggregation Using Intrinsic Tryptophan Fluorescence, *J. Am. Chem. Soc. 48*, 2752−2760.
52. Krishnan, S., Chi, E. Y., Wood, S. J., Kendrick, B. S., Li, C., Garzon-Rodriguez, W., Wypych, J., Randolph, T. W., Narhi, L. O., Biere, A. L., Citron, M., and Carpenter, J. F. (2003) Oxidative dimer formation is the critical rate-limiting step for Parkinson's disease α-synuclein fibrillogenesis, *Biochemistry 42*, 829−837.
53. Kayed, R., Sokolov, Y., Edmonds, B., McIntire, T. M., Milton, S. C., Hall, J. E., and Glabe, C. G. (2004) Permeabilization of lipid bilayers is a common conformation-dependent activity of soluble amyloid oligomers in protein misfolding diseases, *J. Biol. Chem. 279*, 46363−46366.
54. Volles, M. J., and Lansbury, P. T., Jr. (2007) Relationships between the sequence of alpha-synuclein and its membrane affinity, fibrillization propensity, and yeast toxicity, *J. Mol. Biol. 366*, 1510−1522.
55. Rochet, J. C., Outeiro, T. F., Conway, K. A., Ding, T. T., Volles, M. J., Lashuel, H. A., Bieganski, R. M., Lindquist, S. L., and Lansbury, P. T. (2004) Interactions among alpha-synuclein, dopamine, and biomembranes: some clues for understanding neurodegeneration in Parkinson's disease, *J. Mol. Neurosci. 23*, 23−34.
56. Sharma, N., Brandis, K. A., Herrera, S. K., Johnson, B. E., Vaidya, T., Shrestha, R., and Debburman, S. K. (2006) alpha-Synuclein budding yeast model: toxicity enhanced by impaired proteasome and oxidative stress, *J. Mol. Neurosci. 28*, 161−178.

BI701522M